Article

Journal of Vibration and Control
1–14

DOI: 10.1177/1077546315627727
jvc.sagepub.com
SAGE

Natural vibrations of micro beams with nonrigid supports

Diana V Bambill[1,2], Graciela I Guerrero[1,3] and Daniel H Felix[1]

Abstract

The present study aims to provide some new information for the design of micro systems. It deals with free vibrations of Bernoulli–Euler micro beams with nonrigid supports. The study is based on the formulation of the modified couple stress theory. This theory is a nonclassical continuum theory that allows one to capture the small-scale size effects in the vibrational behavior of micro structures. More realistic boundary conditions are represented with elastic edge conditions. The effect of Poisson's ratio on the micro beam characteristics is also analyzed. The present results revealed that the characterization of real boundary conditions is much more important for micro beams than for macro beams, and this is an assessment that cannot be ignored.

Keywords

Micro beam, damage, elastic support, frequency, modified couple stress theory, Ritz, Poisson

1. Introduction

The importance of micro technologies emerges with the necessity of observing, studying, measuring, controlling, manufacturing and manipulation of micro-sized elements. Micro-sized structures and systems (microscopes, super sensitive sensors, high-speed actuators) are widely used in micro-electro-mechanical systems (MEMS; Najar et al., 2010; Ghommem et al., 2013, 2015; Ouakad et al., 2015). Micro structures have the aptitude to survive extreme conditions because of their high-frequency characteristics and high mechanical strength. In particular, micro beams have become important in the fields of MEMS, as well as the study of the small-scale effect on their free vibration modes.

The classical elasticity beam theories have been failed to predict the size dependency of micro structures, because when the magnitudes decrease to micro-scale, many essential phenomena appear that are not significant at macro scales. However, nonlocal theories, which consider additional material length scale constants, have been developed to capture the size dependency of small-sized structures. Within the higher order (nonlocal) theories, there are the micropolar elasticity theory (Cosserat and Cosserat, 1909; Maugin and Metrikine, 2010), Eringen's nonlocal theory (Eringen, 2002) and the strain gradient elasticity and the couple stress theories (Mindlin and Tiersten, 1962; Toupin, 1962). Recently, among several couple stress theories that have been developed, Yang et al. (2002) presented a model based on strain gradient theory. This theory is known as modified couple stress theory. It has a supplementary equilibrium relation to govern the behavior of couples and it involves, besides the Lamè's constants, only one additional material constant. Since 2002 other researchers have developed the modified couple stress theory for the dynamic analysis of Euler–Bernoulli beams: Kong et al. (2008), Şimşek (2010), Asghari et al. (2010) and Wang et al. (2013). Park and Gao (2006) developed a model for the bending of a Bernoulli–Euler beam based on modified couple stress theory that involves only one

[1]Department of Engineering, Institute of Applied Mechanics (IMA), Universidad Nacional del Sur (UNS), Argentina
[2]Consejo Nacional de Investigaciones Científicas y Técnicas (CONICET), Argentina
[3]Faculty of Engineering, Universidad Nacional de la Patagonia San Juan Bosco (UNPSJB), Argentina

Received: 3 June 2015; accepted: 28 December 2015

Corresponding author:
Diana V Bambill, Department of Engineering, Institute of Applied Mechanics, Universidad Nacional del Sur and Consejo Nacional de Investigaciones Científicas y Técnicas, Alem 1253, Bahía Blanca, CP 8000, Argentina.
Email: dbambill@criba.edu.ar

material length scale parameter. They concluded that the bending rigidity of the cantilever beam predicted by their developed model is larger than that predicted by the classical beam model. Araújo dos Santos and Reddy (2012) analyzed the free vibration and buckling of micro beams with a modified couple stress theory taking into account Poisson's effects. Zhang and Fu (2012) developed a new beam model for the viscoelastic micro beam based on the modified couple stress theory. They used it for an electrically actuated micro beam. Akgöz and Civalek (2013) used the Bernoulli–Euler beam and modified couple stress theories together to investigate free vibrations of cantilever micro beams with nonhomogeneous and nonuniform characteristics. They utilized the Rayleigh–Ritz method to carry out the study. Wang et al. (2013) analyzed static bending, post-buckling and free vibration of nonlinear micro beams within the context of nonclassical continuum mechanics, by introducing a material length scale parameter. Ghannadpour et al. (2013) studied the bending, buckling and vibration analyzes of nonlocal Euler beams. They used Ritz method to analyze the nonlocal beams.

On the other hand, it is important to complement the study of free vibrations of micro beams using more realistic representations of support conditions. In general, boundary conditions of micro beams are characterized by classical boundary conditions. However, nonclassical boundary conditions may appear with the real state of supports. Structure support systems probably allow small deflections and/or rotations and so the assumption of a perfect boundary condition will be inadequate. The cause could be that a support is made of noninfinitely rigid material or its foundation may move or there may be minor damage to the supports. Regardless of the cause, unforeseen deformations in supports could affect the natural frequencies of structural systems (Pakdemirli and Boyaci, 2002; Ekici and Boyaci, 2007; Bambill et al., 2013). Not many studies of natural vibrations have analyzed and estimated nonclassical support boundaries of micro-structures. Rinaldi et al. (2008) presented the results of the characterization of nonclassical support boundary conditions of micro cantilevers through electro-mechanical testing. Abadyan et al. (2011) emphasized the importance of characterizing real boundary conditions in design and analysis of NEMS (nano electro mechanical systems). They considered the elastic boundary condition on the nonlinear pull-in behavior of supported NEMS.

Although free vibration analysis of micro beams with the couple stress theory has been presented in the literature, usually the presentations have referred mostly to simply supported, cantilever or double clamped micro beams (bridge): Kong et al. (2008) and Liu and Reddy (2011).

In the present paper free vibrations of micro beams are studied considering the combination of the theories of Bernoulli–Euler and the modified couple stress. The Bernoulli–Euler beam theory takes into account the inertia forces due to transverse translation and ignores the effect of shear deformation and rotatory inertia. The modified couple stress combines a higher order equilibrium relation for moments of couples with the traditional equilibrium relations for forces and moments of forces. The effects of the size dependence are captured by only one additional material length scale parameter. This parameter can be determined from torsion tests of slim cylinders (Chong et al., 2001) or bending tests (Park and Gao, 2006) of thin beams in the micron scale. Chong et al. (2001) analyzed microrod torsion and microplate bending experimental data to determine the magnitude of the strain-gradient material parameters.

In this paper, the application of the couple stress theory in conjunction with the displacement field of a Bernoulli–Euler beam is extended to micro beams with elastic boundary conditions at the ends. It is intended to give additional information for natural vibrations for the appropriate design of micro beams acting in vibrating environments.

In order to demonstrate the validity and accuracy of the present analysis, when it is possible results are compared with previous ones and excellent agreement is observed between them.

1.1. Constitutive micro beam model

The micro beam model is shown in Figure 1. The origin of the Cartesian coordinate system is taken at the left-hand side. The x-axis is considered coincident with the centroidal axis of the beam. The length of the micro beam is L and its volume is $V_b = A \times L$, where $A = b \times h$ is the cross-sectional area. Elastic support boundary conditions are considered at $x = 0$ and $x = L$; they are represented by rotational and translational springs. Those springs are characterized by

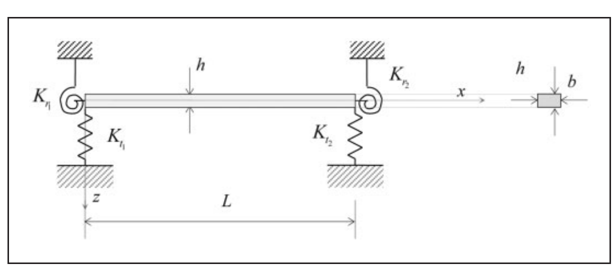

Figure 1. Micro beam with nonrigid boundary conditions and a Cartesian coordinate system.

rotational rigidities: K_{r1} and K_{r2} and translational rigidities K_{t1} and K_{t2}, respectively.

The micro beam executes free transverse vibrations in the x–z plane. Any damping effects are neglected. Although the damping effects are important in studying the behavior over time of a vibrating structure, their influence is minimal in the value of parameters that characterize this behavior, such as natural frequencies and mode shapes. Rayleigh (1877) has shown that undamped systems equations are capable of so-called natural motions. This basically means that all the system coordinates execute harmonic oscillation at a given frequency (natural frequency) and adopt a certain displacement configuration (natural mode shape) (Adhikari, 2000). This is the reason why it is generally accepted not to consider the influence of damping in determining the value of these parameters. As the eminent professor Den Hartog stated in page 40 of his book *Mechanical Vibrations*, referring to the fundamental one-degree-of-freedom-system: '… the natural frequency is practically constant and equal to $\sqrt{k/m}$ for all technical values of damping ($c/c_c < 0.2$' (see Den Hartog, 1956: 40).

2. Formulation

In view of the modified couple stress theory, the strain energy U_1 in a linear elastic isotropic material occupying a volume V_b depends on strain (stress) and curvature (couple stress) (Yang et al., 2002; Park and Gao, 2006):

$$U_1 = \frac{1}{2}\int_{V_b} \left(\sigma_{ij}\varepsilon_{ij} + m_{ij}\chi_{ij}\right) \mathrm{d}V_b \tag{1}$$

where

$$\sigma_{ij} = \lambda\varepsilon_{kk}\delta_{ij} + 2\mu\varepsilon_{ij} \tag{2}$$

are components of the stress tensor, with δ_{ij} the Kronecker's Delta and λ and μ the conventional Lamè's constants.

$$\lambda = \frac{E\nu}{(1+\nu)(1-2\nu)} \qquad \mu = \frac{E}{2(1+\nu)} \tag{3}$$

where ν is the Poisson's ratio and E is the Young's modulus. The shear modulus μ, defined in Equation (3), is also denoted by G in engineering applications.

$$\varepsilon_{ij} = \frac{1}{2}\left(u_{i,j} + u_{j,i}\right) \tag{4}$$

are components of the strain tensor, with u_i components of the displacement vector.

$$m_{ij} = 2l^2\,\mu\,\chi_{ij} \tag{5}$$

are components of the deviatoric part of the symmetric couple stress tensor and l is the material length scale parameter. The value of l depends on and is related to the underlying microstructure of the material; it is a property that considers the effect of couple stress (Mindlin, 1963; Park and Gao, 2006).

$$\chi_{ij} = \frac{1}{2}\left(\theta_{i,j} + \theta_{j,i}\right) \tag{6}$$

are components of the symmetric curvature tensor, and θ_i are components of the rotation vector given by

$$\theta_i = \frac{1}{2} e_{ijk} u_{k,j} \tag{7}$$

where e_{ijk} are the components of the Levi Civita tensor.

Within the context of small strains and small rotations, the displacement field for a Bernoulli–Euler micro beam can be described as

$$u_1 = u(x,t) = -z\frac{\partial w}{\partial x} \; u_2 = \; v(x,t) = 0 \; u_3 = w(x,t) \tag{8}$$

where u is the axial displacement, w is the transverse displacement of the micro beam neutral axis in the z-direction and $\partial w/\partial x$ is the angle of rotation of the centroidal axis of the micro beam. t denotes time.

From Equation (4) and Equations (8) the components of the strain tensor can be written as

$$\boldsymbol{\varepsilon_{ij}} = \begin{bmatrix} \varepsilon_{11} & 0 & 0 \\ 0 & 0 & 0 \\ 0 & 0 & 0 \end{bmatrix} = \begin{bmatrix} -zw'' & 0 & 0 \\ 0 & 0 & 0 \\ 0 & 0 & 0 \end{bmatrix} \tag{9}$$

where $()'$ indicates partial derivation with respect to x: $w' = \frac{\partial w}{\partial x}$, $w'' = \frac{\partial^2 w}{\partial x^2}$.

From Equations (7) and (8) the rotation vector yields

$$\boldsymbol{\theta_i} = [0, -w', 0] \tag{10}$$

Replacing Equation (10) in Equation (6), the curvature tensor takes the form

$$\boldsymbol{\chi_{ij}} = \begin{bmatrix} 0 & \chi_{12} & 0 \\ \chi_{21} & 0 & 0 \\ 0 & 0 & 0 \end{bmatrix} = -\frac{1}{2}\begin{bmatrix} 0 & w'' & 0 \\ w'' & 0 & 0 \\ 0 & 0 & 0 \end{bmatrix} \tag{11}$$

The deviatoric part of the couple stress tensor m_{ij} can be written as

$$\boldsymbol{m_{ij}} = \begin{bmatrix} 0 & m_{12} & 0 \\ m_{21} & 0 & 0 \\ 0 & 0 & 0 \end{bmatrix} = -l^2\mu \begin{bmatrix} 0 & w'' & 0 \\ w'' & 0 & 0 \\ 0 & 0 & 0 \end{bmatrix} \quad (12)$$

Inserting Equation (9) into Equation (2), the stress tensor is obtained:

$$\boldsymbol{\sigma_{ij}} = \begin{bmatrix} \sigma_{11} & 0 & 0 \\ 0 & 0 & 0 \\ 0 & 0 & 0 \end{bmatrix} = (\lambda + 2\mu) \begin{bmatrix} -zw'' & 0 & 0 \\ 0 & 0 & 0 \\ 0 & 0 & 0 \end{bmatrix} \quad (13)$$

where the following expressions apply:

$$\begin{aligned} &\sigma_{11} = (\lambda + 2\mu)(-zw'') \quad \varepsilon_{11} = -zw'' \\ &\chi_{12} = -\frac{1}{2}w'' \quad m_{12} = -E\mu\, w'' \end{aligned} \quad (14)$$

From Equation (1) the strain energy of the micro beam is given by

$$\begin{aligned} U_1 &= \frac{1}{2}\int_0^L (w'')^2 \left[(\lambda + 2\mu)I + l^2\mu A\right]\mathrm{d}x \\ &= \frac{1}{2}\int_0^L (w'')^2\, J\,\mathrm{d}x \end{aligned} \quad (15)$$

The differential volume is written as $dV_b = A\mathrm{d}x$, where $\mathrm{d}x$ is the differential length. $I = \int_A z^2\, \mathrm{d}A$ is the moment of inertia and J is a constant that involves material and geometric characteristics of the micro beam:

$$J = (\lambda + 2\mu)I + \mu A l^2 = \frac{EI(1-\nu)}{(1+\nu)(1-2\nu)} + \frac{EA}{2(1+\nu)} l^2 \quad (16)$$

The potential energy of the boundary support springs is given by

$$\begin{aligned} U_2 = \frac{1}{2}\big[&K_{t_1}(w(0,t))^2 + K_{t_2}(w(L,t))^2 + K_{r_1}(w'(0,t))^2 \\ &+ K_{r_2}(w'(L,t))^2\big] \end{aligned} \quad (17)$$

where K_{t_1}, K_{t_2} and K_{r_1}, K_{r_2} are the translational and rotational spring stiffness constants, respectively (Figure 1).

The kinetic energy of the micro beam can be written as

$$T = \frac{1}{2}\int_0^L \rho A\, (\dot{w})^2\, \mathrm{d}x \quad (18)$$

Here $(\dot{\ })$ indicates partial derivation with respect to time: $\dot{w} = \frac{\partial w}{\partial t}$, and ρ is the material mass density.

Summing Equations (15), (17) and (18) gives the total energy expression:

$$\begin{aligned} \pi = \frac{1}{2}\bigg[&\int_0^L J\,(w'')^2\, \mathrm{d}x + K_{t_1}(w(0,t))^2 + K_{t_2}(w(L,t))^2 \\ &+ K_{r_1}(w'(0,t))^2 + K_{r_2}(w'(L,t))^2 + \int_0^L \rho A\, (\dot{w})^2\, \mathrm{d}x\bigg] \end{aligned} \quad (19)$$

In order to perform a vibration analysis, a harmonic motion is assumed with circular natural frequency, ω. The beam deflection $w(x,t)$ is expressed as

$$w(x,t) = W(x)e^{i\omega t} \quad (20)$$

where W is the mode shape function.

Substituting Equation (20) into Equation (19) results in the following expression:

$$\begin{aligned} \pi = \frac{1}{2}\bigg[&\int_0^L J(W'')^2 e^{i2\omega t}\, \mathrm{d}x + K_{t_1}(W)^2_{x=0}\, e^{i2\omega t} \\ &+ K_{t_2}(W)^2_{x=L}\, e^{i2\omega t} + K_{r_1}\left(W'\right)^2_{x=0} e^{i2\omega t} + K_{r_2}\left(W'\right)^2_{x=L} e^{i2\omega t} \\ &+ \int_0^L \rho A (i\omega)^2 W^2 e^{i2\omega t}\, \mathrm{d}x\bigg] \end{aligned} \quad (21)$$

by applying the principle of minimum energy of the system, the variational expression is obtained:

$$\delta\pi = 0$$

An approximate solution of this variational problem can be found by the Ritz method.

The displacement W is approached as a sum, $W_a(x)$, of trial admissible functions $\psi_j(x)$ with undetermined coefficients C_j:

$$W(x) \cong W_a(x) = \sum_{j=1}^{N} C_j \psi_j(x) \quad (22)$$

where $\psi_j(x)$ represents continuous functions, which depend on x and model the displacement of the micro beam. They satisfy the boundary conditions at the micro beam boundaries.

After introducing Equation (22) into the total energy expression, Equation (21), and minimizing this expression, a system of homogeneous equations of the first order for coefficients C_j is obtained:

$$\frac{\partial \pi}{\partial C_j} = 0 \quad (23)$$

with $j = 1, 2, \ldots, N$.

The natural frequencies correspond to the solutions of the homogeneous form of Equations (23). In order that at least one coefficient be different from zero, it is possible to equate the determinant of this system to zero and obtain the frequency equation:

$$\left|\left[\eta_{i,j}\right] - \omega^2\left[\lambda_{i,j}\right]\right| = 0 \tag{24}$$

The lowest solution, which differs from zero, represents the approximate frequency of the fundamental mode, ω_1, and the following solutions represent the higher frequencies. Dimensionless parameters are assumed to simplify the equations and to compare some particular cases with other authors' results:

$$\bar{x} = \frac{x}{L} \quad k_{t1} = \frac{L^3 K_{t_1}}{J} \quad k_{t2} = \frac{L^3 K_{t_2}}{J} \quad k_{r1} = \frac{L K_{r_1}}{J} \quad k_{r2} = \frac{L K_{r_2}}{J} \tag{25}$$

Moreover, the dimensionless natural frequency parameters are adopted as

$$\Omega_j^2 = \frac{\rho A \omega_j^2}{E\,I} L^4 \tag{26}$$

The expressions of $\eta_{i,j}$ and $\lambda_{i,j}$ in Equation (24) are given by

$$\eta_{i,j} = L^3 \int_0^1 \psi_i(\bar{x})\psi_j(\bar{x})\,\mathrm{d}\bar{x} + k_{t_1}\psi_i(0)\psi_j(0) + k_{r_1} L^2\,\psi_i'(0)\psi_j'(0) + k_{t_2}\,\psi_i(1)\psi_j(1) + k_{r_2}\,L^2 \psi_i'(1)\psi_j'(1) \tag{27}$$

$$\lambda_{i,j} = \frac{1}{L}\int_0^1 \psi_i(\bar{x})\psi_j(\bar{x})\mathrm{d}\bar{x}, \tag{28}$$

where the functions $\psi_j(\bar{x})$ comprise the selected set of admissible functions and satisfy the boundary conditions at both ends of the micro beam (Ilanko et al., 2014). They are adopted as a combination of polynomials:

$$\psi_j(x) = (\bar{x})^{j-1}\ \Psi(\bar{x}) \tag{29}$$

where the function

$$\Psi(\bar{x}) = \alpha_1 \bar{x}^4 + \alpha_2 \bar{x}^3 + \bar{x}^2 + \alpha_3 \bar{x} + \alpha_4$$

has four constants: α_1, α_2, α_3 and α_4, which are determined depending upon the beam boundary conditions at $\bar{x} = 0$ and $\bar{x} = 1$:

$$\Psi''(0) = \frac{L K_{r_1}}{J}\Psi'(0) \quad \Psi'''(0) = -\frac{L^3 K_{t_1}}{J}\Psi(0) \tag{30}$$

$$\Psi''(1) = -\frac{L K_{r_2}}{J}\,\Psi'(1) \quad \Psi'''(1) = \frac{L^3 K_{t_2}}{J}\Psi(1) \tag{31}$$

and they result in

$$\begin{aligned}
\alpha_1 &= \big[12(k_{r1} + k_{r2} + k_{r1}k_{r2})k_{t1} + (12(k_{r1} + k_{r2} + k_{r1}k_{r2}) + (4(3 + k_{r2}) + k_{r1}(4 + k_{r2}))k_{t1})k_{t2}/[24k_{r1}(3 + 2k_{r2})k_{t1} \\
&\quad + k_{r1}(-24(3 + k_{r2}) + (6 + k_{r2})k_{t1})k_{t2}\big] \\
\alpha_2 &= \frac{-48(k_{r1} + k_{r2} + k_{r1}k_{r2})k_{t1} - 2(3(4 + k_{r2}) + k_{r1}(5 + k_{r2}))k_{t1}k_{t2}}{24k_{r1}(3 + 2k_{r2})k_{t1} + k_{r1}(-24(3 + k_{r2}) + (6 + k_{r2})k_{t1})k_{t2}} \\
\alpha_3 &= \frac{2}{k_{r1}} \\
\alpha_4 &= \frac{(288(k_{r1} + k_{r2} + k_{r1}k_{r2}) + 12(3(4 + k_{r2}) + k_{r1}(5 + k_{r2}))k_{t2})}{(24k_{r1}(3 + 2k_{r2})k_{t1} + k_{r1}(-24(3 + k_{r2}) + (6 + k_{r2})k_{t1})k_{t2})}
\end{aligned}$$

As is known, in the modified couple stress theory the parameter J is dependent on the material length scale parameter, on the Poisson's ratio and on the beam thickness and length. Bernoulli–Euler beam theory is valid only when the thickness of the beam is small compared with its length.

3. Analysis of micro beams based on modified couple stress theory

The parameter J of the constitutive micro beam model, based on modified couple stress theory, is given by Equation (16). If a rectangular cross-section is considered (Figure 1), $A/I = 12/h^2$ and J can be written as

$$J = EI\left[(1-\nu) + 6(1-2\nu)/\left({}^{h}/_{l}\right)^2\right] \Big/ [(1+\nu)(1-2\nu)] \tag{32}$$

where the size ratio (h/l) characterizes the thickness dependence of the micro beam on the material length scale parameter and represents the microstructural effect. The material length scale parameter l is thought to be a property of the material and characterized by an empirical constant. However, as Voyiadjis and Abu

Al-Rub (2005) said: '...a fixed value of the material length-scale is not always realistic'. The value of the material length scale parameter may have variations attributed to different manufacturing processes, to different base materials or to different technical equipments. Also, due to the small scale, differences may arise in the experimental techniques to measure the corresponding material length scale parameter. Some values of material properties in the literature are as follows: Epoxy: $E = 1.44\,\text{GPa}$, $\nu = 0.38$ and $l = 17.6\,\mu\text{m}$ (Akgöz and Civalek, 2012); Nickel: $E = 220\,\text{GPa}$, $\nu = 0.26$ and $l = 5\,\mu\text{m}$ (Akgöz and Civalek, 2012); Gold: $E = 79\,\text{GPa}$, $\nu = 0.44$ and $l = 47\,\mu\text{m}$ (Rezazadeh et al., 2012); LIGA Nickel: $E = 165\,\text{GPa}$, $\nu = 0.30$ and $l = 5.6 \pm 0.2\,\mu\text{m}$ (Shrotriya et al., 2003); silicon group 1: $E = 169.2\,\text{GPa}$, $\nu = 0.239$ and $l = 0.58\,\mu\text{m}$; silicon group 2: $E = 130\,\text{GPa}$, $\nu = 0.177$ and $l = 0.71\,\mu\text{m}$ (Osterberg and Senturia, 1997); SU-8 (SU-8 is a commonly used epoxy-based negative photoresist; SU-8 derives its name from the presence of eight epoxy groups): $E = 4.14\,\text{GPa}$ and $l = 1.39\,\mu\text{m}$ (Liebold and Müller, 2015).

The normalized rigidity $J/(EI)$ versus the size ratio of the micro beam based on modified couple stress is plotted as curves in Figure 2. It can be observed that both the size ratio and the Poisson's ratio have an effect on the bending rigidity of the micro beam.

Four different values of Poisson's ratio are considered (i.e., $\nu = 0$, 0.30, 0.38, 0.45). It can be observed that J increases significantly in comparison with the classical EI relation when the beam thickness h is less than or close to the material length scale parameter l. The figure also shows that with $h/l < 1$ the rigidity values of the beam with $\nu = 0$ are larger than those beams with values of ν equal to 0.30, 0.38 and 0.45. Inverse trends are observed for relations of $h/l > 1$.

For a slender beam, the Poisson's effect may be neglected to facilitate the formulation of a simple beam theory; for example, Shames (1985), Park and Gao (2006), Araújo dos Santos and Reddy (2012) and Akgöz and Civalek (2013). By approximating

$$(\lambda + 2\mu)I \cong EI$$

the expression of J, Equation (16), simplifies to

$$J = EI\left[1 + \frac{6}{\left(h/l\right)^2 (1+\nu)}\right] \tag{33}$$

It should be noted that when $h/l \to \infty$, the microstructural effect vanishes and the model is reduced to that of the classical beam theory.

In Figure 3, the parametric curves of J/EI corresponding to Equation (33), versus the size ratio, h/l, are plotted for four different values of ν. Obviously, the Poisson's ratio effect is smaller and the curves of $\nu = 0$, 0.30, 0.38 and 0.45, are closer to each other than in Figure 2.

In both Figures 2 and 3, it can be observed that $\nu = 0$ generates the same plot of $J/(EI)$:

$$J = EI\left[1 + \frac{6}{\left(h/l\right)^2}\right] \tag{34}$$

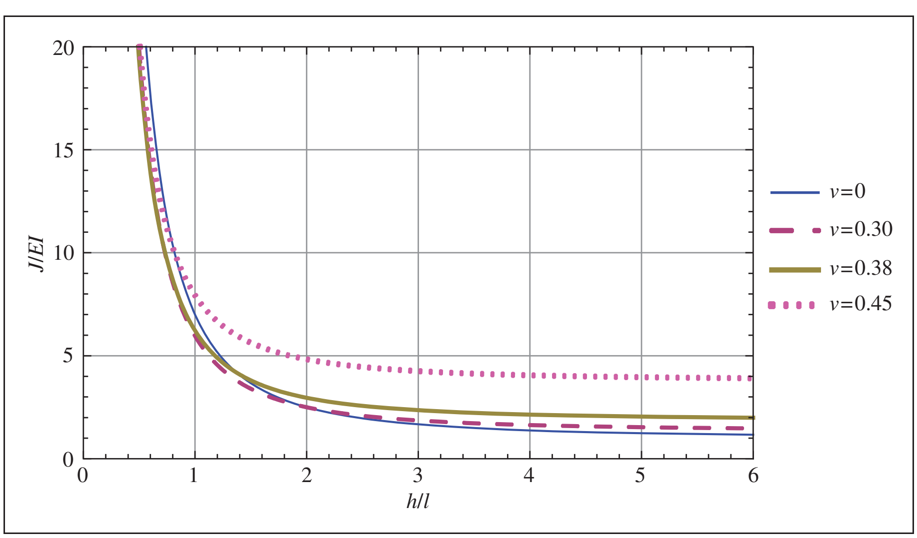

Figure 2. Variation of $J/\left(EI\right) = \left[(1-\nu) + 6(1-2\nu)/\left(h/l\right)^2\right]/\left[(1+\nu)(1-2\nu)\right]$ on $\left(h/l\right)$.

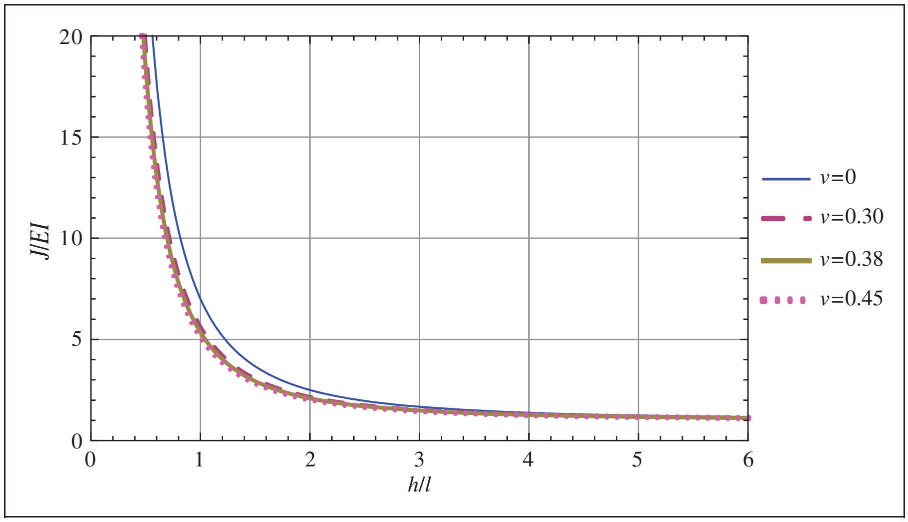

Figure 3. Variation of $J/(EI) = \{1 + 6/[(^h/_l)^2(1+\nu)]\}$ on $^h/_l$.

It can be concluded that the modified couple stress theory's results will change with the increase of the bending rigidity J and that the Poisson's ratio has an effect on it.

4. Numerical results for free vibration

4.1. Poisson's effect

The first example corresponds to a micro beam of rectangular cross-section and classical boundary conditions (simply supported beam: $k_{t1} = k_{t2} \to\infty$, $k_{r1} = k_{r2} \to 0$). The first five natural frequency coefficients are obtained as a function of the size ratio (h/l) for three Poisson's ratios. A comparison can be made only with published results of the fundamental frequency coefficients.

The natural frequency coefficients correspond to $N = 12$ approximation terms. Table 1 shows numerical results of the first five natural frequency coefficients of micro beams with simply supported boundary conditions, by consideration of Equations (32) and (33). Results for $\nu = 0.38$ are compared with the ones obtained by Wang et al. (2013). It can be seen that the obtained results compared fairly well with the published results.

5. Nonrigid boundary conditions

Three cases are presented to show how the modified couple stress theory frequency coefficients change with parameter J (Figures 2 and 3). The cases are defined by the expression of J: (a) the complete expression of J is considered, Equation (32) with $\nu = 0.30$; (b) J is assumed by Equation (33) with $\nu = 0.30$ (Araújo dos Santos and Reddy, 2012); and (c) J is assumed by Equation (34).

The next numerical example corresponds to micro beams characterized by Figure 1. The translational spring constants are assumed to be infinitely rigid, $k_{t1} \to\infty$, $k_{t2} \to\infty$, while the rotational spring constants vary from 0 to infinity. Table 2 shows the first five frequency dimensionless coefficients of Bernoulli–Euler micro beams with elastically restrained boundary conditions for several size ratios $^h/_l$. J comes from Equation (32). Classical boundary support conditions are labeled as SS for simply supported and as C for clamped. Natural frequency coefficients of boundary limiting cases are in total agreement with those of micro beams with classical boundary conditions.

Increments on the boundary condition rigidities produce higher values of the fundamental frequency coefficients; the limiting case $(\to\infty)$ is the infinitely rigid condition. The frequency coefficients predicted by the modified couple stress theory are higher than those predicted by the classical beam theory. As is expected, the natural frequency coefficients calculated for size ratios $h/l \leq 1$ are larger than those calculated by $h/l \in (1, \to\infty)$, as size effects gradually vanish when h/l increases. For h approximately equal to the internal material length scale parameter l, the size effect is remarkably visible.

Table 3 shows results for the limiting case of size ratio $^h/_l \to\infty$. It contains the first five natural frequency coefficients of Bernoulli–Euler beams with elastically restrained boundary conditions. Note that the solution accurately tends to that of the classical Euler–Bernoulli beam. The coefficients correspond to case (b), expression Equation (33) with $\nu = 0.30$. It can be observed that for typical boundary conditions:

Table 1. First five natural frequency coefficients $\Omega_j = \omega_j L^2 \sqrt{\rho A/(E\,I)}$ of simply supported micro beams and three Poisson's ratios.

		$\nu = 0.38$				$\nu = 0.30$		$\nu = 0.25$	
h/l		Eq. (32)	([a])	Eq. (33)	([a])	Eq. (32)	Eq. (33)	Eq. (32)	Eq. (33)
1	Ω_1	24.6142	*24.5891*	22.8237	*22.8004*	24.0978	23.3877	24.1754	23.7691
	Ω_2	98.4569	–	91.2949	–	96.3911	93.5508	96.7015	95.0762
	Ω_3	221.528	–	205.413	–	216.880	210.489	217.578	213.921
	Ω_4	393.828	–	365.179	–	385.564	374.203	386.806	380.305
	Ω_5	615.355	–	570.592	–	602.469	584.717	604.410	594.251
2	Ω_1	16.9772	*16.9598*	14.2579	*14.2433*	15.6052	14.4846	15.2899	14.6389
	Ω_2	67.9087	–	57.0315	–	62.4206	57.9382	61.1594	58.5557
	Ω_3	152.795	–	128.321	–	140.446	130.361	137.609	131.750
	Ω_4	271.635	–	228.126	–	249.682	231.753	244.638	234.223
	Ω_5	424.447	–	356.461	–	390.145	362.129	382.262	365.988
3	Ω_1	15.1461	*15.1306*	12.0194	*12.0071*	13.4566	12.1393	12.9939	12.2213
	Ω_2	60.5843	–	48.0775	–	53.8263	48.5570	51.9755	48.8851
	Ω_3	136.315	–	108.174	–	121.109	109.253	116.945	109.991
	Ω_4	242.337	–	192.310	–	215.305	194.228	207.902	195.540
	Ω_5	378.667	–	300.497	–	336.428	303.494	324.860	305.544
4	Ω_1	14.4505	*14.4357*	11.1301	*11.1187*	12.6185	11.2030	12.0877	11.2531
	Ω_2	57.8019	–	44.5202	–	50.4738	44.8119	48.3508	45.0121
	Ω_3	130.054	–	100.170	–	113.566	100.827	108.789	101.277
	Ω_4	231.207	–	178.081	–	201.895	179.248	193.403	180.048
	Ω_5	361.277	–	278.263	–	315.474	280.086	302.205	281.337
5	Ω_1	14.1169	*14.1025*	10.6934	*10.6825*	12.2111	10.7421	11.6444	10.7755
	Ω_2	56.4676	–	42.7736	–	48.8442	42.9681	46.5776	43.1019
	Ω_3	127.052	–	96.2406	–	109.899	96.6783	104.800	96.9792
	Ω_4	225.870	–	171.094	–	195.377	171.873	186.311	172.407
	Ω_5	352.937	–	267.346	–	305.289	268.562	291.122	269.398
$\to\infty$	Ω_1	13.5036	*13.4898*	9.8696	*9.8595*	11.4511	9.8696	10.8116	9.8696
	Ω_2	54.0143	–	39.4783	–	45.8042	39.4783	43.2463	39.4783
	Ω_3	121.532	–	88.8260	–	103.059	88.8260	97.3040	88.8260
	Ω_4	216.057	–	157.913	–	183.217	157.913	172.985	157.913
	Ω_5	337.603	–	246.749	–	286.288	246.749	270.300	246.749

[a]Wang et al. (2013).

SS-SS, simply supported beam: $k_{t1} \to \infty$, $k_{t2} \to \infty$, $k_{r1} = 0$, $k_{r2} = 0$, the frequency parameters are in total agreement with the known frequency parameters eigenvalues (Blevins, 1979). On the other hand *C-C*, clamped-clamped beam: $k_{t1} \to \infty$, $k_{t2} \to \infty$, $k_{r1} \to \infty$, $k_{r2} \to \infty$, the frequency parameters are in total agreement with the known frequency parameters eigenvalues (Blevins, 1979). The fundamental frequency results Ω_1 are also in excellent agreement with Ghannadpour et al. (2013) for these particular cases.

In Figure 4 a cantilever micro beam of rectangular cross-section is presented. One of the ends of the beam has elastic translational and rotational restrains and the other one is completely free. It can be observed that classical boundary conditions of a clamped-free beam appear when $k_{t1} = k_{r1} \to \infty$. In addition, $k_{t1} = k_{r1} \to 0$ corresponds to the free–free beam. The value of the spring rigidity parameters $k_{t1} = k_{r1}$ of $\to 0$ is treated as equivalent to absence of restrains (free boundary condition); for the limiting case of free–free beams, a zero value is obtained as the first double root of Equation (24) and represents the rigid body motion.

Table 4 contains fundamental frequency coefficients Ω_1 for cantilever micro beams with an elastically clamped condition. The size ratio h/l varies from 0.20 to infinity. Again the modified couple stress theory

Table 2. First five natural frequency coefficients $\Omega_j = \omega_j L^2\sqrt{\rho A/(E\,I)}$ of micro beams with elastically restrained ends, $k_{t1} \to\infty$, $k_{t2} \to\infty$, for various ratios $^h/_l$. Case (a) Equation (32), $\nu = 0.30$ (Figure 1).

$^h/_l$	k_{r1}	k_{r2}	Ω_1	Ω_2	Ω_3	Ω_4	Ω_5	
4	$\to 0$	$\to 0$	11.2030	44.8119	100.827	179.248	280.086	(SS-SS)
		10	14.8650	49.9955	106.868	185.828	287.027	
		100	17.0835	55.4097	115.704	198.016	302.403	
		$\to\infty$	17.5012	56.7146	118.331	202.354	308.786	(SS-C)
	10	10	18.7434	55.1389	112.853	192.355	293.925	
		100	21.2927	60.7592	121.819	204.621	309.343	
		$\to\infty$	21.7873	62.1464	124.529	209.038	315.806	
	100	100	24.2148	66.8580	131.289	217.345	325.180	
		$\to\infty$	24.7944	68.4069	134.213	222.039	331.937	
	$\to\infty$	$\to\infty$	25.3957	70.0034	137.235	226.859	338.895	(C-C)
2	$\to 0$	$\to 0$	14.4846	57.9382	130.361	231.753	362.129	(SS-SS)
		10	18.1804	62.7596	135.727	237.433	368.003	
		100	21.8171	70.8391	148.065	253.617	387.649	
		$\to\infty$	22.6275	73.3274	152.992	261.626	399.233	(SS-C)
	10	10	21.9723	67.5070	141.035	243.069	373.849	
		100	25.9450	75.7143	153.420	259.252	393.453	
		$\to\infty$	26.8608	78.3089	158.451	267.364	405.153	
	100	100	30.5737	84.5044	166.404	275.720	413.463	
		$\to\infty$	31.6649	87.4595	171.756	284.402	425.503	
	$\to\infty$	$\to\infty$	32.8345	90.5083	177.433	293.307	438.154	(C-C)
1	$\to 0$	$\to 0$	23.3877	93.5508	210.489	374.203	584.717	(SS-SS)
		10	26.5703	97.2018	214.319	378.125	588.680	
		100	34.2625	111.700	234.251	402.342	616.450	
		$\to\infty$	36.5358	118.399	247.029	422.434	644.622	(SS-C)
	10	10	29.7372	100.802	218.122	382.030	592.640	
		100	37.6276	115.218	237.903	406.017	620.091	
		$\to\infty$	40.0501	122.100	250.887	426.371	648.603	
	100	100	46.8626	129.727	258.489	428.820	648.226	
		$\to\infty$	49.6944	137.853	271.645	451.069	676.470	
	$\to\infty$	$\to\infty$	53.0164	146.140	286.491	473.584	707.454	(C-C)
0.5	$\to 0$	$\to 0$	43.5380	174.1517	391.8412	696.6065	1088.4928	(SS-SS)
		10	45.6052	176.3046	394.0033	698.7519	1090.5789	
		100	61.9458	203.2326	428.1726	737.8975	1133.5035	
		$\to\infty$	68.0092	220.3834	459.7941	786.2478	1199.7315	(SS-C)
	10	10	47.6568	178.4401	396.1504	700.8765	1092.6554	
		100	63.9428	204.9367	429.7435	739.1984	1134.5144	
		$\to\infty$	70.2262	222.5312	461.9366	788.3663	1201.8028	
	100	100	82.7496	229.0547	465.0435	771.6714	1178.5119	
		$\to\infty$	89.7784	250.7359	496.2315	827.2129	1243.0336	
	$\to\infty$	$\to\infty$	98.6753	271.9696	533.1222	881.1890	1316.2302	(C-C)

Table 3. First five natural frequency coefficients $\Omega_j = \omega_j L^2 \sqrt{\rho A/(E\,I)}$ of beams with elastically restrained ends, $k_{t1} \to\infty$, $k_{t2} \to\infty$. Case (b) Equation (33) $\nu = 0.30$, $h/l \to\infty$, $J \approx EI$ (Figure 1).

h/l	k_{r1}	k_{r2}	Ω_1	Ω_2	Ω_3	Ω_4	Ω_5	
$\to\infty$	$\to 0$	$\to 0$	9.8696	39.4783	88.8260	157.9130	246.7490	*(SS-SS)*
			9.8696	–	–	–	–	Ghannadpour et al. (2013)
			9.8696	39.4784	88.8264	*157.914*	*246.740*	Blevins (1979)
		10	13.4296	44.7214	95.0921	164.8540	254.1590	
		100	15.1257	49.0446	102.3840	175.1740	267.4420	
		$\to\infty$	15.4181	49.9643	104.2470	178.2700	272.0350	*(SS-C)*
			15.4182	–	–	–	–	Ghannadpour et al. (2013)
			15.4182	*49.9649*	*104.2474*	*178.2697*	*272.031*	Blevins (1979)
	10	10	17.2695	49.9595	101.3160	171.7440	261.5230	
		100	19.2721	54.5090	108.7700	182.1750	274.8810	
		$\to\infty$	19.6272	55.4996	110.7070	185.3440	279.5460	
	100	100	21.5417	59.4473	116.6640	193.0470	288.6590	
		$\to\infty$	21.9517	60.5449	118.7560	196.4130	293.5540	
	$\to\infty$	$\to\infty$	22.3731	61.6715	120.9020	199.8590	298.5620	*(C-C)*
			22.3733	–	–	–	–	Ghannadpour et al. (2013)
			22.3733	*61.7061*	*120.903*	*199.859*	*298.556*	Blevins (1979)

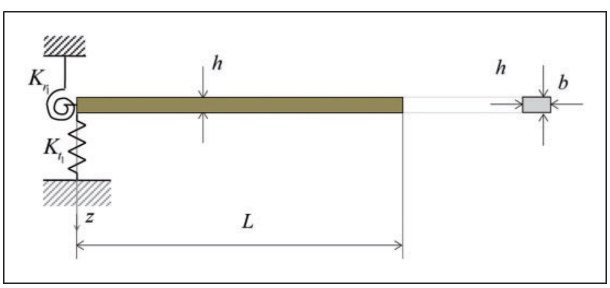

Figure 4. Cantilever micro beam with elastically restrained boundary conditions.

converges to the classical elasticity theory as h/l approaches to infinity (classical Bernoulli–Euler beam theory). The effect of the size ratio h/l on the fundamental frequency parameters can be appreciated in this table. Differences between coefficients of cases (a) and (b) are smaller, <3%, until $h/l \le 1$ and they increase to $\sim$14% for $h/l \to\infty$. In all the relations, coefficients of case (a) are greater than those of case (b). Comparing coefficients calculated with case (a) and (c), it is observed that they are practically equal for $h/l = 2$. For $h/l < 2$ coefficients of case (c) are greater than those of case (a) and for $h/l > 2$ they are smaller. The differences in the frequency coefficients are between 12% and (–16%) with respect to case (c).

On the other hand, it can be observed that case (c) presents higher coefficients than those of case (b) for $h/l \le 4$ and they are nearly the same when $h/l \to\infty$. It is observed that when $k_{t1} = k_{r1} \to\infty$ the agreement with Araújo dos Santos and Reddy (2012) is excellent.

In Table 5 it can be observed how the natural fundamental frequency of a cantilever beam (infinitely rigid clamped condition) diminishes as the support becomes less rigid (becomes more flexible). Then as the boundary condition becomes more flexible, the fundamental frequency is reduced. The more flexible the boundary condition, the lower the frequency.

For example, if $k_{r1} = k_{t1} = 100$ the reduction is 5.5% for the macro beam. For micro beams of different micro size ratios, the reduction is much more significant; for $k_{r1} = k_{t1} = 100$ and $h/l = 1$, it is 24% lower than the same micro beam with the infinitely rigid clamped condition; for $h/l = 0.75$, the frequency is 33% lower and for $h/l = 0.20$, the frequency is almost 72% lower and so on.

Tables 6–8 present the decrement of the boundary rigidities related to the higher frequency values.

Small damage to the supports can generate significant reductions in the fundamental frequency of beams. If k_{t1} and k_{r1} are extremely large the natural fundamental frequency approaches the fundamental frequency $\omega_{1Cantilever}$ of the cantilever beam, with an infinitely rigid condition. $\varepsilon_1 = \frac{\omega_1}{\omega_{1Cantilever}} \times 100 = 100\%$ corresponds to the classical clamped boundary condition.

Table 4. Fundamental frequency coefficients $\Omega_1 = \omega_1 L^2 \sqrt{\rho A/(E\,I)}$ of cantilever micro beams of cases (a), (b) and (c), with the elastic boundary conditions (Figure 4).

	h/l								
$k_{r1} = k_{t1}$	0.20	0.25	0.50	0.75	1.00	1.33	2.00	4.00	$\to\infty$
			(a)	Eq. (32);	$\nu = 0.30$				
$\to 0$	0	0	0	0	0	0	0	0	0
1	0.88802	0.88792	0.88716	0.88604	0.88474	0.88298	0.87999	0.87569	0.87305
10	2.80315	2.80007	2.77604	2.74158	2.70239	2.65052	2.56634	2.45372	2.38925
100	10.7180	9.99765	8.23006	7.21448	6.43758	5.69267	4.85354	4.10381	3.78233
1000	32.5228	27.0400	14.9074	10.5476	8.39534	6.86102	5.48753	4.45338	4.04791
10,000	37.6999	30.2832	15.5885	10.8380	8.56733	6.96969	5.55225	4.49108	4.07625
$\to\infty$	37.9877	30.4885	15.6483	10.8663	8.58478	6.98113	5.55930	4.49529	4.07941
			(b)	Eq. (33);	$\nu = 0.30$				
$\to 0$	0	0	0	0	0	0	0	0	0
1	0.88802	0.88792	0.88714	0.88596	0.88453	0.88248	0.87868	0.87238	0.86790
10	2.80313	2.80003	2.77546	2.73911	2.69605	2.63611	2.53101	2.37350	2.27357
100	10.7136	9.98521	8.20758	7.15789	6.33282	5.52307	4.58466	3.71203	3.32252
1000	32.4840	26.9977	14.7853	10.3613	8.15483	6.55903	5.10008	3.96166	3.49752
10, 000	37.6406	30.2149	15.4522	10.6403	8.31539	6.65719	5.15414	3.98810	3.51426
$\to\infty$	37.9313	30.4183	15.5110	10.6676	8.33182	6.66760	5.16009	3.99104	3.51601
	–	–	–	–	*8.3318*[a]	–	*5.1601*[a]	–	*3.5160*[a]
			(c)	Eq. (34)					
$\to 0$	0	0	0	0	0	0	0	0	0
1	0.88806	0.88799	0.88737	0.88643	0.88526	0.88350	0.87999	0.87336	0.86790
10	2.80442	2.80201	2.78278	2.75357	2.71774	2.66548	2.56634	2.39671	2.27357
100	11.2185	10.3910	8.52161	7.51481	6.71290	5.88369	4.85355	3.81667	3.32288
1000	36.1784	30.0933	16.6036	11.6087	9.07660	7.21956	5.48748	4.09033	3.49819
10, 000	42.8548	34.3727	17.5045	11.9747	9.28190	7.34153	5.55225	4.11962	3.51428
$\to\infty$	43.2054	34.6287	17.5800	12.0095	9.30249	7.35426	5.55930	4.12289	3.51601

[a]Araújo dos Santos and Reddy (2012).

Table 5. Damage to the supports, measured in percentage change rates of the first natural frequency with respect to the cantilever beam (*C-F*), $\varepsilon_1 = {}^{\omega_1}/_{\omega_{1Cantilever}} \times 100$.

Micro beam	$k_{r1} = k_{t1}$					
$^{h}/_{l}$	$\to\infty$	10,000	1000	100	10	1
0.20	100%	99.23%	85.64%	28.24%	7.39%	2.34%
0.25	100%	99.33%	88.75%	32.83%	9.21%	2.92%
0.50	100%	99.62%	95.32%	52.91%	17.89%	5.72%
0.75	100%	99.74%	97.13%	67.10%	25.68%	8.31%
1.00	100%	99.80%	97.88%	76.01%	32.36%	10.62%
1.33	100%	99.84%	98.37%	82.83%	39.54%	13.24%
2.00	100%	99.88%	98.84%	88.85%	49.05%	17.03%
4.00	100%	99.93%	99.26%	93.01%	59.47%	21.86%
$\to\infty$	100%	99.95%	99.47%	94.50%	64.66%	24.68%

Table 6. Damage to the supports, measured in percentage change rates of the second natural frequency with respect to the cantilever beam (*C-F*), $\varepsilon_2 = {}^{\omega_2}/_{\omega_{2Cantilever}} \times 100$.

Micro beam	$k_{r1} = k_{t1}$					
$^h/_l$	$\rightarrow\infty$	10,000	1000	100	10	1
0.20	100%	99.14%	84.68%	16.43%	5.12%	1.64%
0.25	100%	99.21%	86.65%	18.71%	6.33%	2.04%
0.50	100%	99.42%	91.47%	26.74%	11.74%	3.98%
0.75	100%	99.51%	93.07%	32.22%	15.88%	5.73%
1.00	100%	99.56%	93.85%	36.93%	18.92%	7.26%
1.33	100%	99.59%	94.43%	42.36%	21.77%	8.93%
2.00	100%	99.62%	95.11%	50.23%	25.14%	11.23%
4.00	100%	99.66%	95.90%	59.71%	28.81%	13.93%
$\rightarrow\infty$	100%	99.68%	96.33%	64.75%	30.83%	15.39%

Table 7. Damage to the supports, measured in percentage change rates of the third natural frequency with respect to the cantilever beam (*C-F*), $\varepsilon_3 = {}^{\omega_3}/_{\omega_{3Cantilever}} \times 100$.

Micro beam	$k_{r1} = k_{t1}$					
$^h/_l$	$\rightarrow\infty$	10,000	1000	100	10	1
0.20	100%	99.05%	83.09%	38.79%	36.54%	36.29%
0.25	100%	99.10%	84.13%	39.78%	36.69%	36.31%
0.50	100%	99.25%	86.90%	44.12%	37.77%	36.43%
0.75	100%	99.31%	88.04%	46.64%	39.11%	36.61%
1.00	100%	99.35%	88.75%	48.13%	40.40%	36.82%
1.33	100%	99.37%	89.34%	49.44%	41.82%	37.12%
2.00	100%	99.40%	90.20%	51.13%	43.61%	37.64%
4.00	100%	99.43%	91.38%	53.42%	45.40%	38.42%
$\rightarrow\infty$	100%	99.45%	92.05%	54.95%	46.24%	38.93%

Table 8. Damage to the supports, measured in percentage change rates of the fourth natural frequency with respect to the cantilever beam (*C-F*), $\varepsilon_4 = {}^{\omega_4}/_{\omega_{4Cantilever}} \times 100$.

Micro beam	$k_{r1} = k_{t1}$					
$^h/_l$	$\rightarrow\infty$	10,000	1000	100	10	1
0.20	100%	98.95%	81.23%	52.37%	51.15%	51.03%
0.25	100%	98.99%	81.58%	52.97%	51.23%	51.03%
0.50	100%	99.07%	82.41%	56.07%	51.82%	51.10%
0.75	100%	99.12%	82.90%	58.18%	52.60%	51.19%
1.00	100%	99.14%	83.36%	59.40%	53.42%	51.30%
1.33	100%	99.16%	83.78%	60.33%	54.38%	51.46%
2.00	100%	99.18%	84.56%	61.23%	55.72%	51.75%
4.00	100%	99.21%	85.88%	62.05%	57.18%	52.19%
$\rightarrow\infty$	100%	99.23%	86.66%	62.48%	57.89%	52.49%

A damaged support loses rigidity and affects the natural frequencies of structures.

6. Conclusions

The boundary characterization of micro beams is taken into account by rotational and translational springs located at the ends of the beam. The fact of considering elastic boundary conditions allows representing more real support conditions and then, for those cases, determining the corresponding natural frequency values. The Poisson's ratio effect on the bending rigidity of micro beams can be observed, and its influence on the natural frequencies appreciated.

The results indicate that regardless of the cause, unforeseen flexibility in supports affects the natural frequencies of structural systems. In the case of micrometer beams, the effects on the lower frequencies are much more noticeable than in macro-scale beams. In general higher frequencies are less affected than lower frequencies.

To conclude, the characterization of real boundary conditions is much more important for micro-scale beams than for macro-scale beams, and this is an assessment that cannot be ignored.

Declaration of Conflicting Interests

The author(s) declared no potential conflicts of interest with respect to the research, authorship, and/or publication of this article.

Funding

The author(s) disclosed receipt of the following financial support for the research, authorship, and/or publication of this article: This work was supported by Universidad Nacional del Sur (UNS), Consejo Nacional de Investigaciones Científicas y Técnicas (CONICET) and Comisión de Investigaciones Científicas de la Provincia de Buenos Aires (CIC), Argentina.

Acknowledgments

The authors are grateful to the anonymous reviewers for their helpful and valuable comments.

References

Abadyan MR, Beni YT and Noghrehabadi A (2011) Investigation of elastic boundary condition on the pull-in instability of beam-type NEMS under van der Waals attraction. *Procedia Engineering* 10: 1724–1729.

Adhikari S (2000) *Damping models for structural vibration*. PhD Thesis, Cambridge University, UK.

Akgöz B and Civalek O (2012) Analysis of micro-sized beams for various boundary conditions based on the strain gradient elasticity theory. *Archive of Applied Mechanics* 82: 423–443.

Akgöz B and Civalek O (2013) Free vibration analysis of axially functionally graded tapered Bernoulli-Euler microbeams based on the modified couple stress theory. *Composite Structures* 98: 314–322.

Araújo dos Santos JA and Reddy J (2012) Free vibration and buckling analysis of beams with a modified couple-stress theory. *International Journal Applied Mechanics* 04: 1250026–1-28.

Asghari M, Ahmadian MT, Kahrobaiyan MH, et al. (2010) On the size dependent behavior of functionally graded micro-beams. *Materials and Design* 31(5): 2324–2329.

Bambill DV, Rossit CA, Rossi RE, et al. (2013) Transverse free vibration of non uniform rotating Timoshenko beams with elastically clamped boundary conditions. *Meccanica* 48(6): 1289–1311.

Blevins R (1979) *Formulas for natural frequency and mode shape*. New York: Van Nostrand Reinhold.

Chong ACM, Yang F, Lam DCC, et al. (2001) Torsion and bending of micron-scaled structures. *Journal of Materials Research* 16: 1052–1058.

Cosserat E and Cosserat F (1909) *Theory of deformable bodies* (Translated by Delphenich DH.). Paris: Scientific Library, Herman and Sons.

Den Hartog JP (1956) *Mechanical vibrations*, 4th ed. New York: McHill Book Company, Inc.

Ekici HO and Boyaci H (2007) Effects of non-ideal boundary conditions on vibrations of microbeams. *Journal of Vibration and Control* 13(9–10): 1369–1378.

Eringen AC (2002) *Nonlocal continuum field theories*. New York: Springer.

Ghannadpour SAM, Mohammadi B and Fazilati J (2013) Bending, buckling and vibration problems of nonlocal Euler beams using Ritz method. *Composite Structures* 96: 584–589.

Ghommem M, Calo VM and Claudel CG (2015) Micro-cantilever flow sensor for small aircraft. *Journal of Vibration and Control* 21(10): 2043–2058.

Ghommem M, Nayfeh AH and Choura S (2013) Model reduction and analysis of a vibrating beam microgyroscope. *Journal of Vibration and Control* 19(8): 1240–1249.

Ilanko S, Monterrubio LE and Morris R (2014) *The Rayleigh-Ritz method for structural analysis*. London: Wiley & Sons.

Kong S, Zhou S, Nie Z, et al. (2008) The size-dependent natural frequency of Bernoulli–Euler micro-beams. *International Journal of Engineering Science* 46(5): 427–437.

Liebold C and Müller WH (2015) Applications of strain gradient theories to the size effect in submicro-structures incl. Experimental analysis of elastic material parameters. *Bulletin of TICMI* 19(1): 45–55.

Liu YP and Reddy JN (2011) A nonlocal curved beam model based on a modified couple stress theory. *International Journal of Structural Stability and Dynamics* 11(3): 495–512.

Maugin GA and Metrikine AV (eds) (2010) ''Mechanics of generalized continua: one hundred years after the Cosserats''. *Advances in Mechanics and Mathematics*. Vol. 21, New York: Springer.

Mindlin RD and Tiersten HF (1962) Effects of couple-stresses in linear elasticity. *Archive for Rational Mechanics and Analysis* 11(1): 415–448.

Mindlin RD (1963) Influence of couple-stresses on stress concentrations. *Experimental Mechanics* 3(1): 1–7.

Najar F, Nayfeh AH, Abdel-Rahman EM, et al. (2010) Dynamics and global stability of beam-based electrostatic microactuators. *Journal of Vibration and Control* 16(5): 721–748.

Osterberg PM and Senturia SD (1997) M-TEST: a test chip for MEMS material property measurement using electrostatically actuated test structures. *Journal of Microelectromechanical Systems* 6(2): 107–118.

Ouakad HM, Nayfeh AH, Choura S and Najar F (2015) Nonlinear feedback controller of a microbeam resonator. *Journal of Vibration and Control* 21(9): 1680–1697.

Pakdemirli M and Boyaci H (2002) Effect of non-ideal boundary conditions on the vibrations of continuous systems. *Journal of Sound and Vibration* 249(4): 815–823.

Park SK and Gao XL (2006) Bernoulli–Euler beam model based on a modified couple stress theory. *Journal of Micromechanics and Microengineering* 16(1): 2355–2359.

Rayleigh and Lord (1877) *Theory of sound* (two volumes), Reissued 1945, 2nd ed. New York: Dover Publications.

Rezazadeh G, Vahdat AS, Tayefeh-rezaei S, et al. (2012) Thermoelastic damping in a micro-beam resonator tunable with piezoelectric layers. *Acta Mechanica* 223(6): 1137–1152.

Rinaldi G, Packirisamy M and Stiharu I (2008) Boundary characterization of MEMS structures through electromechanical testing. *Sensors and Actuators A* 143(2): 415–422.

Shames IH (1985) *Energy and finite element methods in structural mechanics*. New York: Hemisphere Pub.

Shrotriya P, Allameh SM, Lou J, et al. (2003) On the measurement of the plasticity length scale parameter in LIGA nickel foils. *Mechanics of Materials* 35: 233–243.

Şimşek M (2010) Dynamic analysis of an embedded microbeam carrying a moving micro particle based on the modified couple stress theory. *International Journal of Engineering Science* 48(12): 1721–1732.

Toupin RA (1962) Elastic materials with couple-stresses. *Archive for Rational Mechanics and Analysis* 11(1): 385–414.

Voyiadjis GZ and Abu Al-Rub RK (2005) Gradient plasticity theory with a variable length scale parameter. *International Journal of Solids and Structures* 42: 3998–4029.

Wang YG, Lin WH and Liu N (2013) Nonlinear free vibration of a microscale beam based on modified couple stress theory. *Physica E* 47: 80–85.

Yang F, Chong ACM, Lam DCC, et al. (2002) Couple stress based strain gradient theory for elasticity. *International Journal of Solids and Structures* 39(10): 2731–2743.

Zhang J and Fu Y (2012) Pull-in analysis of electrically actuated viscoelastic micro beams based on a modified couple stress theory. *Meccanica* 47(7): 1649–1658.